Inorg. Chem. **2002**, *41*, 2975–2980

Kinetics and Mechanisms of the Ozone/Bromite and Ozone/Chlorite Reactions

Jeffrey S. Nicoson, Lu Wang, Robert H. Becker, Kara E. Huff Hartz, Charles E. Muller, and Dale W. Margerum*

Department of Chemistry, Purdue University, West Lafayette, Indiana 47907-1393

Received December 20, 2001

Ozone reactions with XO_2^- (X = Cl or Br) are studied by stopped-flow spectroscopy under pseudo-first-order conditions with excess XO_2^-. The O_3/XO_2^- reactions are first-order in $[O_3]$ and $[XO_2^-]$, with rate constants $k_1^{Cl} = 8.2(4) \times 10^6$ M^{-1} s^{-1} and $k_1^{Br} = 8.9(3) \times 10^4$ M^{-1} s^{-1} at 25.0 °C and $\mu = 1.0$ M. The proposed rate-determining step is an electron transfer from XO_2^- to O_3 to form XO_2 and O_3^-. Subsequent rapid reactions of O_3^- with general acids produce O_2 and OH. The OH radical reacts rapidly with XO_2^- to form a second XO_2 and OH^-. In the O_3/ClO_2^- reaction, ClO_2 and ClO_3^- are the final products due to competition between the OH/ClO_2^- reaction to form ClO_2 and the OH/ClO_2 reaction to form ClO_3^-. Unlike ClO_2, BrO_2 is not a stable product due to its rapid disproportionation to form BrO_2^- and BrO_3^-. However, kinetic spectra show that small but observable concentrations of BrO_2 form within the dead time of the stopped-flow instrument. Bromine dioxide is a transitory intermediate, and its observed rate of decay is equal to half the rate of the O_3/BrO_2^- reaction. Ion chromatographic analysis shows that O_3 and BrO_2^- react in a 1/1 ratio to form BrO_3^- as the final product. Variation of k_1^X values with temperature gives $\Delta H^{\ddagger}_{Cl} = 29(2)$ kJ mol^{-1}, $\Delta S^{\ddagger}_{Cl} = -14.6(7)$ J mol^{-1} K^{-1}, $\Delta H^{\ddagger}_{Br} = 54.9(8)$ kJ mol^{-1}, and $\Delta S^{\ddagger}_{Br} = 34(3)$ J mol^{-1} K^{-1}. The positive $\Delta S^{\ddagger}_{Br}$ value is attributed to the loss of coordinated H_2O from BrO_2^- upon formation of an $[O_3BrO_2^-]^{\ddagger}$ activated complex.

Introduction

The reactions of ozone with halite ions XO_2^- (X = Cl or Br) are important in the formation of bromate and chlorate ions, which are hazardous disinfection byproducts.[1] Ozone is known to behave as both an electron acceptor (with $IrCl_6^{3-}$)[2] and an oxygen-atom donor (with SO_3^{2-}, I^-, and Br^-).[3] The reaction between O_3 and ClO_2^- was studied by Emerich[4] and by Klaning, Sehested, and Holcman.[5] Emerich[4] found that the stoichiometry of the reaction was consistent with a combination of eqs 1 and 2. His study also showed that, as the ratio $[ClO_2^-]/[O_3]$ increases to about 200, the production of ClO_2 becomes nearly quantitative and ClO_3^- is no longer an appreciable product of the reaction.

$$O_3 + 2ClO_2^- + H_2O \rightarrow 2ClO_2 + O_2 + 2OH^- \quad (1)$$

$$O_3 + ClO_2^- \rightarrow ClO_3^- + O_2 \quad (2)$$

Klaning, Sehested, and Holcman[5] used stopped-flow spectroscopy under second-order conditions to study the O_3/ClO_2^- reaction and proposed a mechanism that involves an initial electron-transfer reaction between O_3 and ClO_2^- to form O_3^- and ClO_2 in the rate-determining step. The authors concluded that further rapid reactions of O_3^- occur to form O_2 and OH radical, and the OH radical reacts rapidly with ClO_2^- to form ClO_2 or with ClO_2 to form ClO_3^-. They used a trial and error method in conjunction with a simulation program to determine a rate constant of $(4 \pm 1) \times 10^6$ M^{-1} s^{-1} for the initial electron-transfer step. The trial and error method was necessary because fitting kinetic data for second-order reactions requires knowledge of the stoichiometry of the reaction. However, the competitive nature of the OH/

* Author to whom correspondence should be addressed. E-mail: margerum@purdue.edu.

(1) (a) Karpel vel Leitner, N.; DeLaat, J.; Dore, M.; Suty, H. In *Disinfection Byproducts in Water Treatment*; Minear, R. A., Amy, G. L., Eds.; CRC Press: Boca Raton, FL, 1996; pp 393−406. (b) von Gunten, U.; Hoigne, J. In *Disinfection Byproducts in Water Treatment*; Minear, R. A., Amy, G. L., Eds.; CRC Press: Boca Raton, FL, 1996; pp 187−206.
(2) Bennett, L. E.; Warlop, P. *Inorg. Chem.* **1990**, *29*, 1975−1981.
(3) Liu, Q.; Schurter, L. M.; Muller, C. E.; Aloisio, S.; Francisco, J. S.; Margerum, D. W. *Inorg. Chem.* **2001**, *40*, 4436−4442.
(4) Emerich, D. E. Ph.D. Thesis, Miami University, Miami, OH, 1981.
(5) Klaning, U. K.; Sehested, K.; Holcman, J. *J. Phys. Chem.* **1985**, *89*, 760−763.

10.1021/ic011301s CCC: $22.00
Published on Web 04/26/2002

ClO_2^- and OH/ClO_2 reactions ensures that exact knowledge of the stoichiometry can never be obtained, because it will vary throughout the course of the reaction.

Several authors[6−9] have suggested that the reaction of O_3 and BrO_2^- has a rate constant greater than 10^5 M^{-1} s^{-1}, although a direct determination was not made. The mechanism of the O_3/BrO_2^- reaction has not been previously discussed. The present work uses stopped-flow spectroscopy under pseudo-first-order conditions to relate the rate constants, activation parameters, and mechanisms of the oxidation of ClO_2^- and BrO_2^- by O_3.

Experimental Section

Reagents. Doubly deionized, distilled water was used for all solution preparations. Stock solutions of $NaClO_4$ were prepared from the recrystallized salt. $NaBrO_2$ (29.9 wt %) was prepared as previously reported[10] and contained NaOH (20.7%), $NaNO_3$ (4.2%), Na_2SO_4 (41.6%), $NaBrO_3$ (3.2%), and NaBr (0.3%) impurities. The BrO_2^- solutions were standardized spectrophotometrically at 295 nm ($\epsilon_{BrO_2^-} = 115$ M^{-1} cm^{-1}).[11,12] Commercial $NaClO_2$ was purified as previously reported, and the solutions were standardized spectrophotometrically at 260 nm ($\epsilon_{ClO_2^-} = 154$ M^{-1} cm^{-1}).[13] Solutions of O_3 were prepared by passing research grade oxygen through a 9 kV, 30 mA ozone generator. The O_3 solutions were standardized spectrophotometrically at 260 nm ($\epsilon_{O_3} = 3290$ M^{-1} cm^{-1}).[14]

Methodology and Instrumentation. The measured pH was converted to $p[H^+]$ on the basis of electrode calibration at $\mu = 1.0$ M ($NaClO_4$). Kinetic data for the O_3/XO_2^- reactions were obtained under pseudo-first-order conditions observing the loss of O_3 at 260 nm on the Applied PhotoPhysics stopped flow (APPSF) spectrophotometer model SX-18MV (cell path 0.962 cm). Observed rate constants (k_{obsd}) greater than 100 s^{-1} were corrected for the mixing efficiency of the APPSF spectrophotometer on the basis of the calibration of the instrument with well-characterized reaction systems.[15] For the O_3/BrO_2^- reaction, at least a 10-fold excess of $[BrO_2^-]$ over $[O_3]$ was used. Simulations of the kinetic data for the O_3/BrO_2^- reaction were performed using Specfit ver. 2.1 with a Runge−Kutta numerical integration.

The O_3/ClO_2^- reaction was so fast that it approached the limits of the APPSF instrument. To obtain the pseudo-first-order rate constants, a 2−10-fold initial excess of $[ClO_2^-]$ over $[O_3]$ was used so that the rate of the reaction was slow enough to measure. The latter portion of the data, where the ratio $[ClO_2^-]/[O_3]$ becomes greater than 10, was fit to an exponential equation to give k_{obsd}. For instance, when the initial ratio $[ClO_2^-]/[O_3]$ is 4/1 and assuming that at most two ClO_2^- ions are consumed for every O_3 molecule, the ratio becomes 10/1 after 2 half-lives. In most cases, the time required to achieve a 10/1 ratio was within the dead time of the APPSF instrument (2−3 ms) and the reaction was observed in a 3−60 ms time period. The final concentration of ClO_2^- was used to extract the second-order rate constant. The value of $[ClO_2^-]_f$ was calculated from the final absorbance at 260 nm, by taking into account the absorbance due to ClO_2 formed from the reaction ($\epsilon_{ClO_2} = 60$ M^{-1} cm^{-1}). The final ClO_2 concentration was determined from separate pushes that monitored the reaction at 359 nm, where only ClO_2 absorbs significantly ($\epsilon_{ClO_2} = 1230$ M^{-1} cm^{-1}).[13]

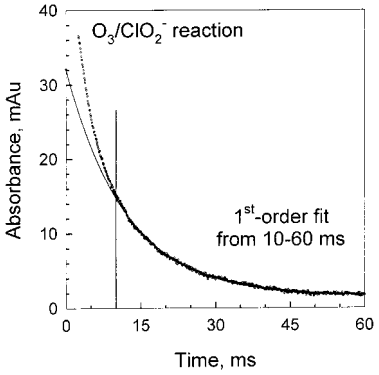

Figure 1. Kinetic trace for the O_3/ClO_2^- reaction ($[O_3]_i = 26.7$ μM, $[ClO_2^-]_i = 55.8$ μM, $[H_2PO_4^-]_T = 50$ mM, $p[H^+]$ 6.00, $\mu = 1.0$ M ($NaClO_4$), 25.0 °C, $\lambda = 260$ nm, path length 0.962 cm). The solid line is the exponential fit to the data after pseudo-first-order conditions are attained, 10 ms.

Chromatographic data were collected for the products of the O_3/BrO_2^- reaction by using a Dionex DX-500 HPLC instrument. Samples were injected through a 25 μL injection loop to quaternary amine anion exchange guard and separation columns. The analytes were eluted with 9.0 mM Na_2CO_3 at a 1 mL/min flow rate and were detected by conductivity detection after background suppression with an ASRS-Ultra suppressor with a self-regenerating current of 100 mA.

Results and Discussion

Kinetics of the O_3/XO_2^- Reaction. Under pseudo-first-order conditions, the O_3/BrO_2^- reaction shows a first-order loss in absorbance from O_3 at 260 nm. Figure 1 shows that the rapid O_3/ClO_2^- reaction also fits an exponential decay in the later stages of the reaction when the ratio $[ClO_2^-]/[O_3]$ becomes 10/1. As the concentration of XO_2^- (X = Cl or Br) increases, k_{obsd} increases with a first-order dependence on $[XO_2^-]$ (Figure 2a,b). This is consistent with the rate expression in eq 3 for the loss of O_3. The least-squares slope

$$-d[O_3]/dt = k_1^X[XO_2^-][O_3] = k_{obsd}^X[O_3] \qquad (3)$$

of the data in plots a and b of Figure 2 gives rate constants of $k_1^{Cl} = 8.2(4) \times 10^6$ M^{-1} s^{-1} and $k_1^{Br} = 8.9(3) \times 10^4$ M^{-1} s^{-1} at 25.0 °C. The observed rate constants do not vary with $p[H^+]$ or phosphate buffer concentration (p S1 of the Supporting Information). The value of k_1^{Cl} determined in the present work is more reliable than the value reported previously[5] because the use of pseudo-first-order conditions does not require a trial and error method in the determination of the rate constant. For the O_3/BrO_2^- reaction, the assumption made by several authors[6−9] that k_1^{Br} is greater than 10^5 M^{-1} s^{-1} is not correct.

In the present study, the kinetics of the O_3/XO_2^- reactions are examined at many wavelengths. For the O_3/ClO_2^-

(6) Haag, W. R.; Hoigne, J. *Environ. Sci. Technol.* **1983**, *17*, 261−267.
(7) von Gunten, U.; Hoigne, J. *Environ. Sci. Technol.* **1994**, *28*, 1234−1242.
(8) von Gunten, U.; Oliveras, Y. *Environ. Sci. Technol.* **1998**, *32*, 63−70.
(9) Pinkernell, U.; von Gunten, U. *Environ. Sci. Technol.* **2001**, *35*, 2525−2531.
(10) Wang, L.; Nicoson, J. S.; Huff Hartz, K. E.; Francisco, J. S.; Margerum, D. W. *Inorg. Chem.* **2002**, *41*, 108−113.
(11) Perrone, T. F. Ph.D. Thesis, Purdue University, West Lafayette, IN, 1999.
(12) Lee, C. L.; Lister, M. W. *Can. J. Chem.* **1979**, *57*, 1524−1530.
(13) Furman, C. S.; Margerum, D. W. *Inorg. Chem.* **1998**, *37*, 4321−4327.
(14) Hart, E. J.; Sehested, K.; Holcman, J. *Anal. Chem.* **1983**, *55*, 46−49.
(15) Nicoson, J. S.; Margerum, D. W. *Inorg. Chem.* **2002**, *41*, 342−347.

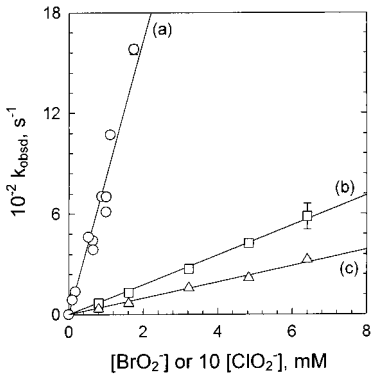

Figure 2. Dependence of the first-order rate constant for the O_3/XO_2^- reaction on XO_2^- concentration: (a) O_3/ClO_2^- reaction ($[O_3]_i$ = 26.7−59.5 μM, $[H_2PO_4^-]_T$ = 0.050 M, p[H^+] 6.00, μ = 1.0 M ($NaClO_4$), 25.0 °C, λ = 260 nm for the loss of O_3, slope 8.2(4) × 10^6 M^{-1} s^{-1}); (b) O_3/BrO_2^- reaction ($[O_3]_i$ = 20−100 μM, $[H_2PO_4^-]_T$ = 0.10 M, p[H^+] 6.5(1), μ = 1.0 M ($NaClO_4$), 25.0 °C, λ = 260 nm for the loss of O_3, slope 8.9(3) × 10^4 M^{-1} s^{-1}); (c) same conditions as (b) except λ = 475 nm for the loss of BrO_2 and the slope is 4.8(3) × 10^4 M^{-1} s^{-1}. Observed rate constants were obtained from an average of five pushes except for (c), where only one push was used.

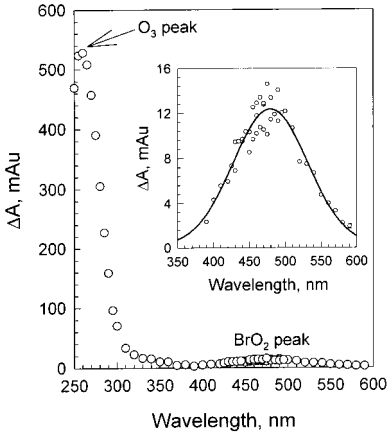

Figure 3. Dependence of the wavelength on the absorbance change for the O_3/BrO_2^- reaction ($[O_3]_i$ = 0.16 μM, $[BrO_2^-]$ = 1.86 mM, $[H_2PO_4^-]_T$ = 0.10 M, p[H^+] 6.40, μ = 1.0 M ($NaClO_4$), 10.0 °C, path length 0.962 cm). To account for O_3 volatility, the data were collected in sets of 10 pushes with at least one overlapping wavelength in each set. The absorbance values were normalized to the same initial O_3 concentration on the basis of the O_3 absorbance at 260 nm. Inset: BrO_2 peak with a Gaussian fit centered at 478 nm.

reaction, the formation of ClO_2 at 359 nm is observed, and the rate constants obtained from these data are similar to those obtained for the loss of O_3 at 260 nm. For the O_3/BrO_2^- reaction, an exponential decay in absorbance is seen in the 450−500 nm range. A plot of the change in absorbance versus wavelength for kinetic data at 10.0 °C (after all data have been normalized to a known initial O_3 concentration) shows a peak at 478 nm (Figure 3). These data are taken at 10.0 °C as opposed to 25.0 °C to decrease the volatility of ozone and maintain its initial concentration as much as possible. The spectrum in Figure 3 is similar to the known spectrum of the BrO_2 radical in aqueous solution (λ_{max} = 475 nm, ϵ = 1000 M^{-1} cm^{-1}).[16] These data indicate that a BrO_2 intermediate is formed rapidly (within the dead time of the APPSF instrument) and appears to decay by a first-order process. A plot of k_{obsd} (475 nm) versus $[BrO_2^-]$ appears to have a first-order dependence on $[BrO_2^-]$, with a slope equal to $^1/_2k_1^{Br}$ at 25.0 °C (Figure 2c).

Products of the O_3/XO_2^- Reaction. For the O_3/ClO_2^- reaction, the products are O_2, ClO_2, and ClO_3^-. As the ratio $[ClO_2^-]_i/[O_3]_i$ is increased to greater than 200, a 2/1 stoichiometric ratio of ClO_2 produced to O_3 consumed is approached. This observation shows that a direct oxygen-atom transfer from O_3 to ClO_2^-, which would produce only ClO_3^- and O_2, is not appreciable. These findings are in agreement with the previous study by Emerich[4] and are consistent with the combination of eqs 1 and 2 when $[ClO_2^-]_i/[O_3]_i$ is less than 200.

The O_3/BrO_2^- reaction proceeds through 10^{-5} M levels of a BrO_2 intermediate to form O_2 and BrO_3^- as the final products. Ion chromatographic analysis of the products (p S2 of the Supporting Information) gives $\Delta[BrO_2^-]/\Delta[BrO_3^-]$ = 1.06(7), which corresponds to the stoichiometry in eq 4.

$$O_3 + BrO_2^- \rightarrow O_2 + BrO_3^- \quad (4)$$

Mechanism of the O_3/ClO_2^- Reaction. Data for the O_3/ClO_2^- reaction are consistent with the mechanism proposed by Klaning, Sehested, and Holcman (eqs 5−9).[5]

$$O_3 + ClO_2^- \underset{k_{-1}^{Cl}}{\overset{k_1^{Cl}}{\rightleftharpoons}} O_3^- + ClO_2 \quad (5)$$

$$O_3^- + H_2PO_4^- \underset{k_{-2}}{\overset{k_2}{\rightleftharpoons}} HO_3 + HPO_4^{2-} \quad (6)$$

$$HO_3 \xrightarrow{k_3} O_2 + OH \quad (7)$$

$$OH + ClO_2^- \xrightarrow{k_4^{Cl}} OH^- + ClO_2 \quad (8)$$

$$OH + ClO_2 \xrightarrow{k_5^{Cl}} H^+ + ClO_3^- \quad (9)$$

One minor modification to their mechanism is made for the decomposition of O_3^- in eqs 6 and 7, which is assisted by $H_2PO_4^-$.[17] The reactions in eqs 6−9 are much more rapid than the k_{-1}^{Cl} step, and the loss of O_3 is governed by k_1^{Cl}. Since ClO_2 is a stable product that builds up to an appreciable concentration compared to ClO_2^-, competition between eq 8 (k_4^{Cl} = 4.2 × 10^8 M^{-1} s^{-1})[5] and eq 9 (k_5^{Cl} = 4.0 × 10^8 M^{-1} s^{-1})[5] determines the final products. Thus, the stoichiometry for the O_3/ClO_2^- reaction is consistent with eq 1 early in the reaction when little ClO_2 has formed. As the reaction proceeds and the concentration of ClO_2 increases, the contribution of k_5^{Cl} becomes greater and a mixture of ClO_2 and ClO_3^- results. Since the number of moles of ClO_2^- consumed for every mole of O_3 varies as the reaction proceeds, analysis under second-order conditions is not valid. Therefore, the value determined in this work under pseudo-first-order conditions represents a more accurate determination of k_1^{Cl}. All of the rate constants are provided in Table

(16) Buxton, G. V.; Dainton, F. S. *Proc. R. Soc. London, A* **1968**, *304*, 427−439.

(17) Buhler, R. E.; Staehelin, J.; Hoigne, J. *J. Phys. Chem.* **1984**, *88*, 2560−2564.

Table 1. Summary of Rate Constants for the O_3/XO_2^- Reactions[a]

rate constant	O_3/BrO_2^-	O_3/ClO_2^-	rate constant	O_3/BrO_2^-	O_3/ClO_2^-
k_1^X, $M^{-1}\ s^{-1}$	$8.9(3) \times 10^4$ [b]	$8.2(4) \times 10^6$ [b]	k_3, s^{-1}	1.1×10^5 [e]	1.1×10^5 [e]
k_{-1}^X, $M^{-1}\ s^{-1}$	4.6×10^9 [c]	1.8×10^5 [d]	k_4^X, $M^{-1}\ s^{-1}$	1.9×10^9 [f]	4.2×10^8 [d]
k_2, $M^{-1}\ s^{-1}$	2.1×10^8 [e]	2.1×10^8 [e]	k_5^X, $M^{-1}\ s^{-1}$		4.0×10^8 [d]
k_{-2}, $M^{-1}\ s^{-1}$	2.0×10^7 [e]	2.0×10^7 [e]	k_{BrO_2}, $M^{-1}\ s^{-1}$	5×10^7 [g]	

[a] Conditions: 25.0 °C; $\mu = 1.0$ M. [b] This work. [c] Determined using the k_1^{Br} from this work and $K_1^{Br} = 1.92 \times 10^{-5}$ calculated from the reduction potentials in refs 5 and 10. [d] Reference 17. [e] Reference 5. [f] Reference 16. [g] This work, 10 °C.

1. The values of k_{-1}^{Cl}, k_2, k_{-2}, k_3, k_4^{Cl}, and k_5^{Cl} were determined previously by pulsed-radiolysis methods.[5,17]

Mechanism of the O_3/BrO_2^- Reaction. Analysis of the products shows that O_3 and BrO_2^- react in a 1/1 ratio to form O_2 and BrO_3^-. These data seem to validate a one-step oxygen-atom-transfer mechanism (eq 4). Also, the one-electron reduction potentials for O_3 ($E° = 1.01$ V)[5] and BrO_2 ($E° = 1.289$ V)[10] show that an initial electron-transfer step to form O_3^- and BrO_2 is not very favorable ($E°_{O_3/BrO_2^-} = -0.288$ V). However, the detection of a BrO_2 intermediate in the O_3/BrO_2^- reaction provides excellent evidence for the existence of an electron-transfer pathway. The following mechanism is proposed to account for the observed kinetics, stoichiometry, and BrO_2 intermediate:

$$O_3 + BrO_2^- \underset{k_{-1}^{Br}}{\overset{k_1^{Br}}{\rightleftharpoons}} O_3^- + BrO_2 \qquad (10)$$

$$O_3^- + H_2PO_4^- \underset{k_{-2}}{\overset{k_2}{\rightleftharpoons}} HO_3 + HPO_4^{2-} \qquad (6)$$

$$HO_3 \xrightarrow{k_3} O_2 + OH \qquad (7)$$

$$OH + BrO_2^- \xrightarrow{k_4^{Br}} OH^- + BrO_2 \qquad (11)$$

$$BrO_2 + BrO_2 \underset{k_{-6}}{\overset{k_6}{\rightleftharpoons}} Br_2O_4 \qquad (12)$$

$$Br_2O_4 + H_2O \xrightarrow{k_7} BrO_2^- + BrO_3^- + 2H^+ \qquad (13)$$

The combination of eqs 6, 7, 10, and 11 gives the stoichiometry for the formation of BrO_2 (eq 14). The k_1^{Br} step is the rate-determining step for the overall process in eq 14, and the rate expression for the formation of BrO_2 is given in eq 15.

$$O_3 + 2BrO_2^- + 2H^+ \rightarrow O_2 + 2BrO_2 + H_2O \qquad (14)$$

$$d[BrO_2]/dt = 2k_1^{Br}[BrO_2^-][O_3] = 2k_{obsd}[O_3] \qquad (15)$$

In the O_3/BrO_2^- mechanism, a OH/BrO_2 reaction (analogous to the k_5 step (eq 9) for the O_3/ClO_2^- system) is excluded because BrO_2 ($\sim 10^{-5}$ M) does not build up to a concentration comparable to that of BrO_2^- ($\sim 10^{-3}$ M). Buxton and Dainton[16] determined a value of $1.9 \times 10^9\ M^{-1}\ s^{-1}$ for k_4^{Br}. Since the OH/BrO_2 rate constant can be no larger than the diffusion limit of $10^{10}\ M^{-1}\ s^{-1}$, this reaction is negligible compared to the OH/BrO_2^- reaction in eq 11.

The BrO_2 radical decays by its disproportionation in aqueous solution to form BrO_2^- and BrO_3^- (eqs 12 and 13). Although 2 mol of BrO_2^- are consumed in the formation of BrO_2 (eq 14), 1 mol of BrO_2^- is released in the decay of BrO_2, and the overall reaction reduces to the experimentally determined stoichiometry in eq 4. Previous reports on the disproportionation of BrO_2 under acidic[18] and basic[16] conditions show that the reaction proceeds by formation of a Br_2O_4 dimer followed by hydrolysis of Br_2O_4. Field and Forsterling[18] determined $k_6 = 1.4 \times 10^9\ M^{-1}\ s^{-1}$, $k_{-6} = 7.4 \times 10^4\ s^{-1}$, and $k_7 = 2.2 \times 10^3\ s^{-1}$ at 20.0 °C in 1 M H_2SO_4. Since k_{-6} is larger than k_7, the decay of BrO_2 can be approximated by the preequilibrium rate expression in eq 16, where $k_7k_6/k_{-6} = k_{BrO_2}$.

$$-{}^1/_2\ d[BrO_2]/dt = k_{BrO_2}[BrO_2]^2 = (4.2 \times 10^7)[BrO_2]^2 \qquad (16)$$

Since BrO_2 is an intermediate in the O_3/BrO_2^- reaction, its concentration is expected to rise to a maximum and then fall to zero. However, since eq 16 involves a squared dependence on $[BrO_2]$, the sum of eqs 15 and 16 gives a nonlinear differential equation that cannot be easily integrated. The experimental data at 475 nm (where only BrO_2 absorbs) show an exponential decay with an observed rate constant that is linearly dependent on $[BrO_2^-]$ (Figure 2c). These data indicate that the maximum concentration of BrO_2 is reached within the dead time of the stopped-flow instrument and that *the subsequent loss of BrO_2 is governed by the rate expression for its formation* (eq 15). This statement appears illogical since the decay of BrO_2 is known to be second-order, not first-order. However, this situation is similar to kinetic systems involving consecutive first-order reactions (eq 17). When $k_b > k_a$, the loss of B after its

$$A \xrightarrow{k_a} B \xrightarrow{k_b} C \qquad (17)$$

maximum concentration has been reached is proportional to $k_a[A]$.[19−21] A similar kinetic behavior was found in an earlier study[19] of the formation and decay of a highly reactive Cu^{III} intermediate where the rate of decay was actually governed by the rate of formation of the intermediate.

Plot c of Figure 2 shows that the rate constant for the loss of BrO_2 is half the rate constant for the loss of O_3. However, if the loss of BrO_2 were governed by eq 15, the rate constant for BrO_2 would be expected to be a factor of 2 larger, not smaller, than the rate constant for O_3. This disparity can be explained by identifying an expression for the maximum

(18) Field, R. J.; Forsterling, H.-D. *J. Phys. Chem.* **1986**, *90*, 5400−5407.
(19) Gray, E. T., Jr.; Taylor, R. W.; Margerum, D. W. *Inorg. Chem.* **1977**, *16*, 3047−3055.
(20) Alcock, N. W.; Benton, D. J.; Moore, P. *Trans. Faraday Soc.* **1970**, *66*, 2210−2213.
(21) Espenson, J. H. *Chemical Kinetics and Reaction Mechanisms*, 2nd ed.; McGraw-Hill Inc.: New York, 1995; p 73.

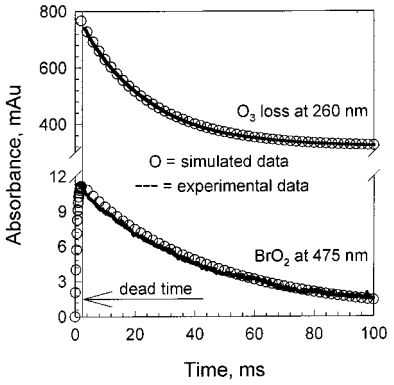

Figure 4. Absorbance versus time for the O_3/BrO_2^- reaction ($[O_3]_i$ = 0.15 mM, $[BrO_2^-]$ = 1.86 mM, $[H_2PO_4^-]_T$ = 0.10 M, p$[H^+]$ 6.40, μ = 1.0 M ($NaClO_4$), 10.0 °C, path length 0.962 cm). The solid lines are the experimental data. The open circles are simulated data points based on the proposed mechanism.

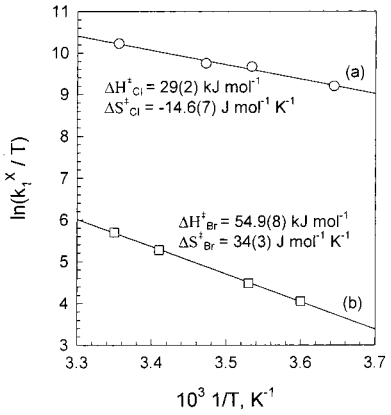

Figure 5. Eyring plots for the O_3/XO_2^- reactions: (a) O_3/ClO_2^-; (b) O_3/BrO_2^-.

concentration of BrO_2 ($[BrO_2]_{max}$) and developing an equation for the subsequent loss of this intermediate. The maximum concentration of BrO_2, defined in eq 18, is reached when the rate of formation (eq 15) and the rate of decay (eq 16) of $[BrO_2]$ are equal. (t_{max} is the time at which the maximum concentration of BrO_2 is reached.) The integrated rate expression for the loss of O_3 (eq 19) is substituted for $[O_3]$ in eq 18 to achieve an integrated equation for $[BrO_2]$ (eq 20). The integrated rate expression in eq 20 confirms that BrO_2 appears to decay with a rate that is half the rate of decay of O_3. As a consequence, the observed decay of BrO_2 is controlled by the rate of its formation.

$$[BrO_2]_{max} = \left(\frac{k_1[O_3][BrO_2^-]}{k_{BrO_2}}\right)_{t_{max}}^{1/2} \quad (18)$$

$$[O_3] = [O_3]_i e^{-k_1[BrO_2^-]t} \quad (19)$$

$$[BrO_2] = \left(\frac{k_1[O_3]_i[BrO_2^-]}{k_{BrO_2}}\right)^{1/2} e^{(-k_1/2)[BrO_2^-]t} \quad (20)$$

A kinetic simulation of the reaction using numerical integration is designed to further test the proposed mechanism. Equations 6, 7, and 11 are rapid steps and do not contribute to the kinetics of the reaction. The reduced kinetic model in eq 21 is used to simulate kinetic data. The model

$$O_3 + BrO_2^- \xrightarrow{k_1^{Br}} 2BrO_2 \xrightarrow{k_{BrO_2}} BrO_3^- \quad (21)$$

in eq 21 uses only those steps that contribute to the kinetics of the reaction, and therefore does not represent the overall stoichiometry of the reaction. Since the spectrum of the BrO_2 intermediate is characterized (Figure 3) by using the kinetic spectra at 10 °C, the value of $k_1^{Br} = 2.50 \times 10^4$ M^{-1} s^{-1} is experimentally determined at this temperature for the simulation. The value of $k_{BrO_2} = k_7k_6/k_{-6}$ is not known under these conditions (10 °C, p$[H^+]$ 6.4, 0.10 M $H_2PO_4^-/HPO_4^{2-}$) and is varied from 10^7 to 10^8 M^{-1} s^{-1} to obtain the best fit to the experimental data.

Figure 4 shows simulated data using the model in eq 21 with $k_{BrO_2} = 5 \times 10^7$ M^{-1} s^{-1}, along with experimental stopped-flow traces for the absorbance of O_3 at 260 nm and BrO_2 at 475 nm. (The experimental absorbances at the two different wavelengths are obtained from separate pushes on the stopped-flow instrument and are normalized to the same initial concentration of O_3. The simulated data for O_3 are adjusted for the background absorbance of the excess BrO_2^-.) A value of $k_{BrO_2} = 5 \times 10^7$ M^{-1} s^{-1} gives the same maximum absorbance due to BrO_2 at 475 nm that is observed experimentally. The simulated data show a rapid increase in absorbance due to BrO_2 within 3 ms and the decay of BrO_2 that accurately mimics the experimental data. The simulated data show that the loss of BrO_2 appears to follow first-order kinetics and that the observed rate constant is a factor of 2 smaller than the rate constant for the loss of O_3. This agrees with the experimental data and the integrated expression in eq 20. Therefore, the kinetic simulation agrees with the proposed mechanism for the O_3/BrO_2^- reaction.

Kinetic simulations are also used to test the possibility of an oxygen-atom-transfer pathway competing with the electron-transfer pathway. Incorporation of this path into the mechanism (50% electron transfer, 50% atom transfer) reduces the maximum concentration of BrO_2 in the simulation by a factor of 2. To force the simulation to agree with the experimental data ($[BrO_2]_{max} = 1.1 \times 10^{-5}$ M), the value of k_{BrO_2} must be reduced. However, this also has the effect of increasing t_{max} to greater than 3 ms. This does not agree with the experimental observation (t_{max} < 3 ms), and we conclude that the oxygen-atom-transfer pathway is at most a minor pathway.

Activation Parameters of the O_3/XO_2^- Reaction. The rate constants for the electron-transfer reaction between O_3 and XO_2^- are determined at various temperatures (pp S3−S6 of the Supporting Information). The plots of $\ln(k_1^X/T)$ versus $1/T$ are straight lines (Figure 5) and yield the activation parameters $\Delta H^{\ddagger}_{Cl} = 29(2)$ kJ mol^{-1}, $\Delta S^{\ddagger}_{Cl} = -14.6(7)$ J mol^{-1} K^{-1}, $\Delta H^{\ddagger}_{Br} = 54.9(8)$ kJ mol^{-1}, and $\Delta S^{\ddagger}_{Br} = 34(3)$ J mol^{-1} K^{-1}.

The values of $\Delta H^{\ddagger}_{Cl}$ and $\Delta S^{\ddagger}_{Cl}$ are consistent with a rapid reaction between O_3 and ClO_2^- to form $[O_3ClO_2^-]^{\ddagger}$ in the transition state. The reaction between O_3 and BrO_2^- to form

an $[O_3BrO_2^-]^‡$ activated complex has a positive $\Delta S^‡_{Br}$ value. We propose that the increase in entropy is due to the loss of H_2O coordinated to BrO_2^- upon formation of the transition state. The difference in $\Delta S^‡_X$ for the O_3/ClO_2^- reaction versus the O_3/BrO_2^- reaction is likely due to greater solvent organization around BrO_2^- than ClO_2^-. The BrO_2^- ion should exhibit stronger interactions with H_2O because of the more polar O−Br bonds as opposed to O−Cl bonds in ClO_2^-.

Comparison of O_3/BrO_2^- and O_3/ClO_2^-. The rate-determining step in both reactions is the transfer of an electron from XO_2^- to O_3 to form XO_2 and O_3^-. This initial step is much more favorable for the O_3/ClO_2^- reaction due to the stability of ClO_2 as opposed to BrO_2 in aqueous solution. Consequently, the rate constant for the O_3/ClO_2^- reaction is almost 2 orders of magnitude larger than that for the O_3/BrO_2^- reaction. The activation parameters for the reactions suggest that H_2O is released upon the formation of $[O_3BrO_2^-]^‡$. This solvent effect is not appreciable for the O_3/ClO_2^- reaction.

Electron-Transfer versus Atom-Transfer Reactions of O_3. The oxidation of many nonmetal species with O_3 occurs by an oxygen-atom-transfer mechanism. This is the case in the O_3 reactions with SO_3^{2-}, I^-, and Br^-,[3] where O_3 behaves as an electrophile and forms an adduct with the SO_3^{2-}, I^-, or Br^- prior to the transfer of an oxygen atom. The relative rates of these reactions correlate with the nucleophilicity of the species oxidized by O_3. In the O_3/XO_2^- reactions, O_3 behaves as an electron acceptor instead of an oxygen-atom donor. In these reactions, the transfer of an electron to form O_3^- and XO_2 provides a lower kinetic barrier than breaking an O−O bond to directly form O_2 and XO_3^-.

Acknowledgment. This work was supported by National Science Foundation Grant CHE-98-18214.

Supporting Information Available: Tables and figures of kinetic data. This material is available free of charge via the Internet at http://pubs.acs.org.

IC011301S